Jet Tomography in Heavy-Ion Collisions with Deep Learning

Yi-Lun Du,[1,*] Daniel Pablos,[2,†] and Konrad Tywoniuk[1,‡]
[1]Department of Physics and Technology, University of Bergen, Postboks 7803, 5020 Bergen, Norway
[2]INFN, Sezione di Torino, via Pietro Giuria 1, I-10125 Torino, Italy

(Received 9 July 2021; accepted 29 November 2021; published 5 January 2022)

Deep learning techniques have the power to identify the degree of modification of high energy jets traversing deconfined QCD matter on a jet-by-jet basis. Such knowledge allows us to study jets based on their initial, rather than final, energy. We show how this new technique provides unique access to the genuine configuration profile of jets over the transverse plane of the nuclear collision, both with respect to their production point and their orientation. By effectively removing the selection biases induced by final-state interactions, one can analyze the potential azimuthal anisotropies of jet production associated to initial-state effects. Additionally, we demonstrate the capability of our new method to locate with precision the production point of a dijet pair in the nuclear overlap region, in what constitutes an important step forward toward the long term quest of using jets as tomographic probes of the quark-gluon plasma.

DOI: 10.1103/PhysRevLett.128.012301

Introduction.—Jets are collimated sprays of hadrons that are produced in hard QCD processes in high-energy particle collisions [1–3]. Within the context of heavy-ion collisions, they are witnesses to the creation of deconfined QCD matter, known as the quark-gluon plasma (QGP), which behaves very close to a perfect liquid [4–6]. During their passage through this medium, partonic jet modes are subject to momentum diffusion and energy loss by the radiation of soft quanta toward large angles, a phenomenon known as jet quenching [7–10]. Key information about the medium is contained in the detailed modification of these hard probes, turning them into essential tools on which tremendous theoretical and experimental effort is being devoted [11–16].

Using jets as differential probes of the spatiotemporal structure of the QGP created in heavy-ion collisions, also known as *jet tomography*, is a long-standing goal [17–22]. On a jet-by-jet basis it is evident that the modifications induced by the medium follow from the local properties sampled along the jet trajectory from the hard production point out to the detector. The ability to unambiguously gauge the effect from the QGP on this level would lead to unprecedented precision in determining local properties of the fluid, including flow [23,24], path-length dependence of modifications [25], and the possibility of observing deconfined quasiparticle degrees of freedom in the QGP [26–28]. Nonetheless, tomographic analyses on the level of inclusive jet populations have been hindered by intrinsic biases that accentuate samples experiencing small modifications over samples that are strongly affected [29]. Such biases arise due to the steeply falling spectrum of the jet initiator transverse momenta and strongly distort the magnitude of medium effects, e.g., the in-medium path-length distribution of surviving jets.

In this Letter we propose a technique, based on deep learning, that mitigates these bias effects and results in better control of the path length traversed by individual jets based on their level of modification. Given a measured jet at p_T and cone size R, the procedure allows us to estimate with reasonable accuracy the transverse momentum p_T^{initial} the jet would have had, had it not interacted with a medium; see Ref. [30] for further details on how to establish such a correspondence. The technique uses only the information of the hadrons that are contained in the reconstructed jet and is easily adaptable to other model studies.

Having at hand an estimate of how much energy an individual jet has lost is a powerful tool that allows for many interesting applications [30]. Here, we demonstrate the usefulness of our approach to tomographic applications in two concrete examples. The first deals with reconstructing the true distribution of path lengths that jets experience, eliminating the effects of "surface bias" [19,20,31] and revealing the potential contributions to jet azimuthal anisotropy that do not stem from final-state interactions. The second application combines the extraction of the lost energy with accessible knowledge about the orientation of the jet with respect to the event plane of the collision, as determined by the dominant azimuthal harmonic v_2 of the particle distribution. This allows one to constrain the path-length dependence separately for jets traveling parallel and transverse to the event plane of the collisions, refining the path to experimentally pin down the original production point of a dijet pair. We expect this new development to importantly contribute to the set of tools aimed at the exploitation of energetic jets as tomographic probes of the QGP.

Quantifying energy loss jet by jet.—In vacuum, high energy partons produced in a hard QCD collision relax their large virtuality down to the hadronization scale via successive splittings. The description of these processes is well controlled both from theory [32–34] and within Monte Carlo parton shower generators [35] through the appropriate implementation of the Dokshitzer–Gribov–Lipatov–Altarelli–Parisi evolution equations. In the medium, the presence of a significant phase space for vacuumlike emissions, occurring before any medium-induced modifications have had the time to develop, has been firmly established [36–38]. The presence of this vacuumlike phase space, which strongly impacts the amount of jet energy loss based on the vacuum-set scales governing jet activity (multiplicity, i.e., number of energy loss sources), is in fact what allows us to understand a great number of jet quenching observables, such as the relative suppression between jets and hadrons [36,39], or the narrowing of the angular opening between the leading groomed subjets [40,41]. In the leading-logarithmic approximation, it is legitimate to assume that the in-cone emissions that belong to the vacuumlike dominated region already define the energy that the jet would have had in the absence of the medium, which we call p_T^{initial}. The presence of the medium alters this fairly developed structure, typically leading to energy loss due to the transport of particles out of the jet cone and defining the jet energy in the medium, or simply p_T.

Within this factorized picture, we can define what we call the energy loss ratio $\chi \equiv p_T/p_T^{\mathrm{initial}}$. In Ref. [30] we describe the matching procedure carried out at the hadron level necessary to establish this connection between a quenched jet and its vacuumlike counterpart. In our previous and current work, we use the hybrid strong-weak coupling model [42–44] for the generation of the quenched jets. We extract χ on a jet-by-jet basis by using jet images as inputs to a convolutional neural network (CNN), achieving a good degree of accuracy across a wide range in χ [45]. We refer the interested readers to our previous paper [30] for further details on data preprocessing and software architecture (see also Ref. [46] for a complementary approach).

Factoring out final-state effects.—In nucleus-nucleus collisions, the production of hard processes can be described by the Glauber model [47,48], where the rate of collisions is governed by the inelastic cross section of nucleon-nucleon scatterings and the density of nucleons are described by the Woods-Saxon distribution. The distribution of production points is naturally strongly correlated with the distribution of path lengths experienced by the entire jet population. However, jets that experience final-state interactions will tend to be more modified, and experience, on average, more energy loss if they originate from production points deep within the nuclear overlap region rather than from the surface. Therefore, selecting a jet population based on their *final*, measured transverse momenta will bias the jet selection toward short path lengths and small energy losses, leading to a "surface bias" [19,20,31]. In contrast, focusing on the original jet population, or selecting jets according to their *initial* transverse momentum, accessed with $p_T^{\mathrm{initial}} = p_T/\chi$, should recover the true path-length distribution associated to the underlying nuclear overlap density.

In order to visualize these aspects, we generate dijet events at $\sqrt{s_{NN}} = 5.02$ TeV for PbPb collisions in the 0–5% centrality bin corresponding to around 700 000 samples of inclusive jets reconstructed with anti-k_t [49] and radius parameter $R = 0.4$ using FastJet [50]. In the left column of Fig. 1 we show the production point density of the hard QCD processes in the transverse plane using three different jet selections. In the top left panel, we select jets with a measured momentum $p_T > 200$ GeV and plot the location where they were produced (taken directly from the model). This selection, referred to as the *final energy selection* (FES), is the only possible setup in experiments without the knowledge of χ. Taking the difference with

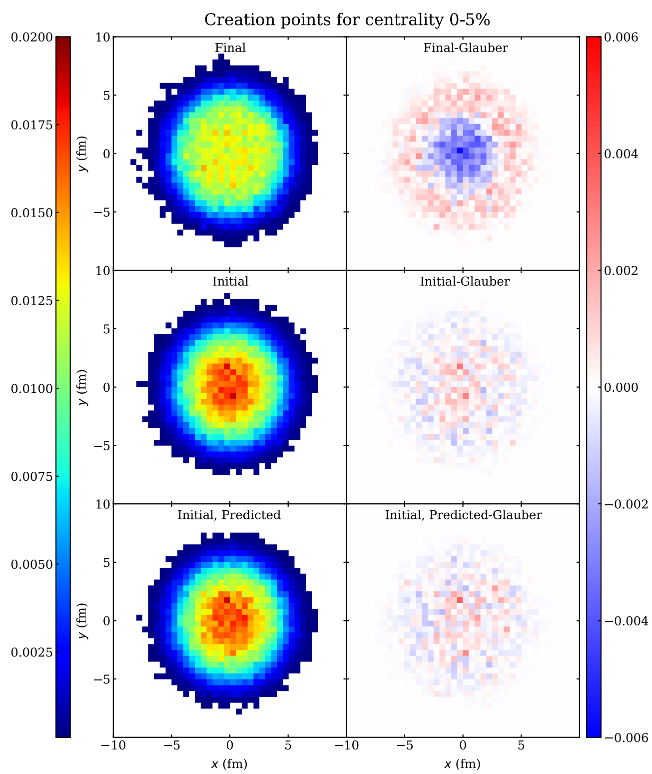

FIG. 1. Left: probability distribution of the production point in the transverse plane of a hard QCD process when using the FES setup, in the top, versus when the IES setup is used, with true χ in the middle and with predicted χ^p in the bottom. Right: difference of the results of the left column with respect to the distribution obtained by directly using the Glauber procedure.

respect to the actual production point density using the Glauber model in the top right plot of Fig. 1 we observe that, compared with the true geometrical distribution according to which the jets were produced, there is a relative absence of jets produced at the center of the overlap region.

With a good estimate of the energy loss ratio χ we can, however, perform a different jet selection. In the middle and bottom left plots of Fig. 1 we show the jet production points (again, supplied by the model) for the so-called *initial energy selection* (IES) with true, i.e., extracted directly from model data, and predicted, i.e., extracted by the trained CNN, χ, respectively, where we only include those jets with $p_T^{\mathrm{initial}} > 200$ GeV [51]. Remarkably, the differences with respect to the Glauber distribution, shown in the middle and bottom right panels, display no sizeable deviation beyond random noise. A detailed error analysis is presented in the Supplemental Material [45]. This demonstrates that, by employing IES, we are able to mitigate almost all final-state effects, such as medium-induced energy loss, and we obtain a jet population that reflects the true path-length distribution experienced in a heavy-ion collision.

Selection bias effects affect not only the creation point distribution in the transverse plane but also the jet orientation with respect to the event plane of the collision [52]. In contrast to the production points shown in Fig. 1, the azimuthal distribution of particle production can be measured in experiments and quantified by the harmonic coefficients $v_n = \langle \exp[i\, n\phi] \rangle$, where ϕ is the azimuthal angle with respect to the event plane and the average is taken over all measured events. In particular, for high-p_T probes, the second harmonic coefficient v_2 is given directly by $v_2 = \langle (p_{T,x}^2 - p_{T,y}^2)/(p_{T,x}^2 + p_{T,y}^2) \rangle$. These momentum anisotropies can emerge both due to initial-state correlations and final-state interactions [53–55]. The former arise from quantum interference in the incoming nuclear wave functions and dominate the observable signal of v_2 only at small multiplicities [56]. The latter are generally driven by the geometry of the collisions (the nuclear positions within the nuclei at a given impact parameter) [57,58].

We show results for jet v_2 from the hybrid strong-weak coupling model in Fig. 2 in PbPb collisions at $\sqrt{s_{NN}} = 5.02$ TeV, using anti-k_t and $R = 0.4$, as a function of centrality. The red dots correspond to the obtained v_2 using FES for jets with measured $p_T > 200$ GeV. (We have checked that the results from the hybrid model reproduce experimental data on high-p_T v_2 at $\sqrt{s_{NN}} = 2.76$ TeV [59] very well; see the Supplemental Material [45] for more details). As the nuclear overlap region becomes more and more anisotropic with increasing impact parameter (increasing the centrality class), final-state energy loss effects increasingly enhance the relative contribution of the less quenched jets that propagate along the short axis of the collision. Thus, v_2^{FES} is positive and grows with centrality. However, as the medium becomes smaller and colder at the most peripheral collisions, energy loss is reduced and v_2^{FES} consistently decreases [57,58].

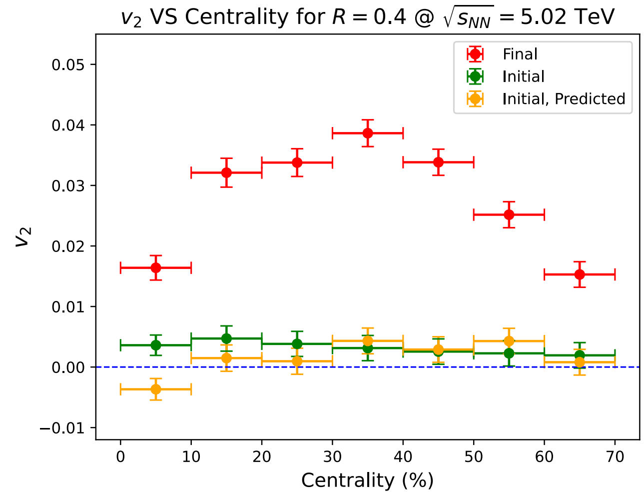

FIG. 2. Centrality dependence of v_2 for FES setup (red) and IES setup with true χ (green) and predicted χ^p (orange).

On the other hand, the green and orange points in Fig. 2 correspond to the results for the IES procedure, using the true and predicted values of χ, respectively, for jets with $p_T^{\mathrm{initial}} > 200$ GeV. By removing the selection bias effect we reveal the initial-state orientation of hard jets in our model which, by construction, is random, and therefore v_2^{IES} is consistent with zero. Remarkably, the agreement between the green and orange dots demonstrates that our algorithm, having been trained on jets in the 0–5% centrality class, is generalizable across a wide range of centrality classes. We also note that our method would have yielded $v_2^{\mathrm{IES}} \neq 0$ and revealed any remaining anisotropy associated to other hypothesized mechanisms, such as quantum correlations in the initial wave functions [60–64] or other quantum interference effects [65–67], although currently known mechanisms are conjectured to average out in large systems due to combinatorial effects. While such effects at high-p_T are expected to be small within current models, finding evidence of such *additional* anisotropies in nucleus-nucleus collisions would support the idea of a common, underlying contribution to collective behavior across different system sizes.

Jet tomography of the QGP.—We now turn to the final application of our tomographic studies using deep learning. Having established that we can restore the true path-length distribution of jets above, we can further narrow down the path-length selection by choosing jets within a class of energy loss ratios, i.e., by choosing jets in a specific range of χ, similar in spirit to the uses of boson-jet selections [20,22] in which the boson energy serves as a proxy for the initial hard parton energy. However, due to the many sources of fluctuations (from jet substructure fluctuations to fluctuations residing in the medium interactions), the correlation between χ and the path length is not as strong as one could have expected [30,69]. Notwithstanding, from

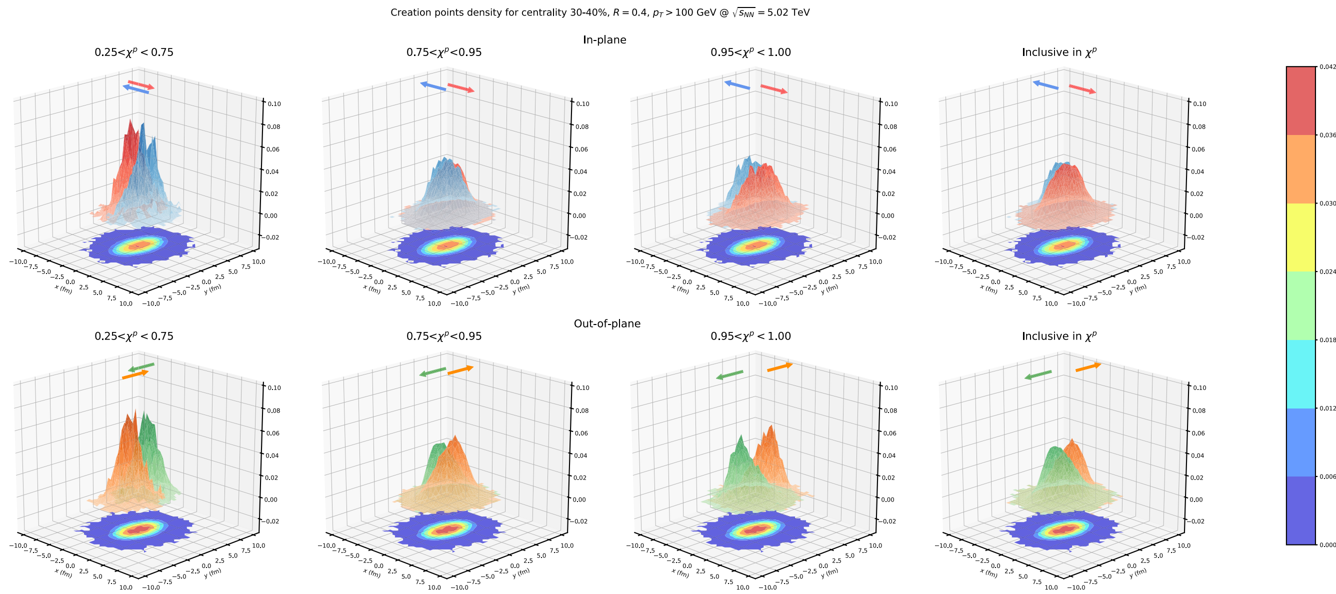

FIG. 3. Creation point distributions in the transverse plane for the jets in 30–40% centrality and inclusive and sliced in different ranges of the predicted χ^p in four columns, respectively. The in plane jets going left (blue) and right (red) are shown in the upper row, and the out of plane jets going up (orange) and down (green) are shown in the lower row. The 2D histogram in the bottom of each plot is the distribution of the inclusive in plane (upper row) and out of plane (lower row) jets in this centrality.

simple geometrical considerations, the path-length distribution and consequently the possible production points in the nuclear overlap area can be constricted further by additionally constricting the direction of the jet propagation with respect to the event plane of the collisions. Concretely, we will consider jets propagating in plane, i.e., parallel to the event plane, and out of plane, i.e., transverse to the event plane.

By combining our knowledge of the orientation of a jet with respect to the event plane with the degree of energy loss χ, we present the localization of the production point of a given jet with a new level of precision. In Fig. 3 we show results for around 900 000 jets, generated at $\sqrt{s_{NN}} = 5.02$ TeV for PbPb collisions at 30–40% centrality and reconstructed using anti-k_t and $R = 0.4$. In the upper (lower) row we have selected jets that are propagating in plane (out of plane), which means they are approximately oriented along the short (long) axis of the nuclear overlap region. This corresponds to jets with distinctly positive (negative) v_2. In the bottom of each subfigure in the upper (lower) row we also plot the average nuclear overlap density, represented by the in plane (out of plane) jet production point distribution for FES inclusive in χ, which has been rotated so that the event plane, and impact parameter vector, points along the x direction. We can further slice the selection depending on which sense the jet is propagating: either left (in blue) or right (in red) for the in plane jets, and either up (in orange) or down (in green) for the out of plane jets. The histograms in each of the first three columns display the creation point density for jets belonging to a given range of the predicted energy loss ratio χ^p. Finally, the fourth column shows the results inclusive in predicted χ^p and corresponds to the production point distributions if we had no knowledge of the degree of in-medium modification.

Even though there is some degree of separation of the production point distributions for the χ-inclusive jet selection, a large degree of overlap can be noticed. This situation changes radically by using our knowledge of predicted χ^p on a jet-by-jet basis [70]. The third column in Fig. 3 shows results for fairly unquenched jets, with $0.95 < \chi^p < 1$. In order to belong to this class, a jet propagating upward (focusing first on the out of plane jets in the lower row) has to have traversed merely a short distance through the QGP, and therefore its production point is predominantly localized in the *upper* part of the overlap region (and vice versa for a jet propagating downward). This reasoning also applies, in reverse, for jets belonging to the very quenched class, with $0.25 < \chi^p < 0.75$, displayed in the leftmost column. In this case, a very quenched jet propagating upward will have needed to traverse a long distance in the QGP, or analogously through a hot region, and consequently its production point will instead be predominantly localized in the *lower* hemisphere (and vice versa for the downward propagating case). Obviously, analogous arguments also apply for the in plane cases plotted in the upper row of Fig. 3. The second column shows the notably overlapping transition region that bridges the gap between the fairly unquenched and very quenched classes of columns 1 and 3, respectively.

Conclusions.—In this Letter, we demonstrate the power of deep learning techniques to pin down the genuine nuclear density distributions that affect high-p_T jet production in the transverse plane and the initial-state jet azimuthal anisotropies, quantifiable through the elliptic flow coefficient v_2, by learning the amount of energy loss χ on a jet-by-jet basis. In both cases, the final-state effects induced by the selection bias can be removed to a large extent by selecting a jet population according to their initial transverse momenta. It would be very interesting to assess the performance and p_T reach of our technique when compared to other methods of obtaining relatively unbiased distributions, such as the quantile procedure [71,72] or the use of boson-jet systems [20,43,72]. We have argued that extracting the possible initial-state anisotropies in nucleus-nucleus collisions can serve to clarify the origin of the high-p_T v_2 measured in small systems, which currently seems in strong conflict with an explanation based solely on energy loss physics. Furthermore, by selecting jets according to the sign of v_2, we have shown the capability of our method to locate with precision the jet creation point in the transverse plane, representing a significant development toward using jets as tomographic probes of the QGP. The interplay between the jet and the local properties of the medium, such as the local hydrodynamic flow [23,24,73–75] or temperature and density gradients [21,22,24], which determine preferred directions and deformed radiation spectra for the soft quanta emitted from the jet, could also be used to greatly improve the prediction performance of χ and even allow for a direct extraction of the traversed length in the QGP. This is a challenging task that will be tackled in future work.

This work is supported by the Trond Mohn Foundation under Grant No. BFS2018REK01 and the University of Bergen. Y. D. thanks the support from the Norwegian e-infrastructure UNINETT Sigma2 for the data storage and HPC resources with Projects No. NS9753K and No. NN9753K. D. P. has received funding from the European Union's Horizon 2020 research and innovation program under the Marie Skłodowska-Curie Grant Agreement No. 754496.

*yilun.du@uib.no
†daniel.pablos.alfonso@to.infn.it
‡konrad.tywoniuk@uib.no

[1] G. P. Salam, Eur. Phys. J. C **67**, 637 (2010).
[2] A. J. Larkoski, I. Moult, and B. Nachman, Phys. Rep. **841**, 1 (2020).
[3] S. Marzani, G. Soyez, and M. Spannowsky, *Looking Inside Jets: An Introduction to Jet Substructure and Boosted-Object Phenomenology* (Springer, New York, 2019), Vol. 958.
[4] K. Ackermann, N. Adams, C. Adler, Z. Ahammed, S. Ahmad, C. Allgower, J. Amsbaugh, M. Anderson, E. Anderssen, H. Arnesen *et al.*, Phys. Rev. Lett. **86**, 402 (2001).
[5] K. Aamodt, B. Abelev, A. A. Quintana, D. Adamova, A. Adare, M. Aggarwal, G. A. Rinella, A. Agocs, S. A. Salazar, Z. Ahammed *et al.*, Phys. Rev. Lett. **105**, 252302 (2010).
[6] K. Aamodt, B. Abelev, A. A. Quintana, D. Adamova, A. Adare, M. Aggarwal, G. A. Rinella, A. Agocs, A. Agostinelli, S. A. Salazar *et al.*, Phys. Rev. Lett. **107**, 032301 (2011).
[7] D. d'Enterria, Landolt-Bornstein **23**, 471 (2010).
[8] A. Majumder and M. Van Leeuwen, Prog. Part. Nucl. Phys. **66**, 41 (2011).
[9] Y. Mehtar-Tani, J. G. Milhano, and K. Tywoniuk, Int. J. Mod. Phys. A **28**, 1340013 (2013).
[10] J.-P. Blaizot and Y. Mehtar-Tani, Int. J. Mod. Phys. E **24**, 1530012 (2015).
[11] B. Abelev *et al.* (ALICE Collaboration), J. High Energy Phys. 03 (2014) 013.
[12] J. Adam *et al.* (ALICE Collaboration), Phys. Lett. B **746**, 1 (2015).
[13] G. Aad, B. Abbott, J. Abdallah, S. A. Khalek, O. Abdinov, R. Aben, B. Abi, M. Abolins, O. AbouZeid, H. Abramowicz *et al.*, Phys. Rev. Lett. **114**, 072302 (2015).
[14] M. Aaboud *et al.* (ATLAS Collaboration), Phys. Lett. B **774**, 379 (2017).
[15] M. Aaboud, G. Aad, B. Abbott, O. Abdinov, B. Abeloos, D. K. Abhayasinghe, S. H. Abidi, O. AbouZeid, N. Abraham, H. Abramowicz *et al.*, Phys. Lett. B **790**, 108 (2019).
[16] S. Acharya *et al.* (ALICE Collaboration), Phys. Rev. C **101**, 034911 (2020).
[17] E. Wang and X.-N. Wang, Phys. Rev. Lett. **89**, 162301 (2002).
[18] T. Renk, Phys. Rev. C **74**, 034906 (2006).
[19] H. Zhang, J. F. Owens, E. Wang, and X.-N. Wang, Phys. Rev. Lett. **98**, 212301 (2007).
[20] H. Zhang, J. F. Owens, E. Wang, and X.-N. Wang, Phys. Rev. Lett. **103**, 032302 (2009).
[21] Y. He, L.-G. Pang, and X.-N. Wang, Phys. Rev. Lett. **125**, 122301 (2020).
[22] W. Chen, Z. Yang, Y. He, W. Ke, L.-G. Pang, and X.-N. Wang, Phys. Rev. Lett. **127**, 082301 (2021).
[23] N. Armesto, C. A. Salgado, and U. A. Wiedemann, Phys. Rev. C **72**, 064910 (2005).
[24] A. V. Sadofyev, M. D. Sievert, and I. Vitev, arXiv:2104.09513.
[25] B. Betz and M. Gyulassy, J. High Energy Phys. 08 (2014) 090; 10 (2014) 043(E).
[26] F. D'Eramo, K. Rajagopal, and Y. Yin, J. High Energy Phys. 01 (2019) 172.
[27] J. a. Barata, Y. Mehtar-Tani, A. Soto-Ontoso, and K. Tywoniuk, Phys. Rev. D **104**, 054047 (2021).
[28] M. Cè, T. Harris, H. B. Meyer, and A. Toniato, J. High Energy Phys. 03 (2021) 035.
[29] R. Baier, Y. L. Dokshitzer, A. H. Mueller, and D. Schiff, J. High Energy Phys. 09 (**2001**) 033.
[30] Y.-L. Du, D. Pablos, and K. Tywoniuk, J. High Energy Phys. 03 (2021) 206.
[31] A. Dainese, C. Loizides, and G. Paic, Eur. Phys. J. C **38**, 461 (2005).
[32] M. Dasgupta, F. Dreyer, G. P. Salam, and G. Soyez, J. High Energy Phys. 04 (2015) 039.
[33] M. Dasgupta, F. A. Dreyer, G. P. Salam, and G. Soyez, J. High Energy Phys. 06 (**2016**) 057.
[34] Z.-B. Kang, F. Ringer, and I. Vitev, J. High Energy Phys. 10 (2016) 125.
[35] S. Alioli *et al.*, arXiv:1902.01674.

[36] Y. Mehtar-Tani and K. Tywoniuk, Phys. Rev. D **98**, 051501 (R) (2018).

[37] P. Caucal, E. Iancu, A. H. Mueller, and G. Soyez, Phys. Rev. Lett. **120**, 232001 (2018).

[38] F. Domínguez, J. G. Milhano, C. A. Salgado, K. Tywoniuk, and V. Vila, Eur. Phys. J. C **80**, 11 (2020).

[39] J. Casalderrey-Solana, Z. Hulcher, G. Milhano, D. Pablos, and K. Rajagopal, Phys. Rev. C **99**, 051901(R) (2019).

[40] J. Casalderrey-Solana, G. Milhano, D. Pablos, and K. Rajagopal, J. High Energy Phys. 01 (2020) 044.

[41] P. Caucal, E. Iancu, and G. Soyez, J. High Energy Phys. 10 (2019) 273.

[42] J. Casalderrey-Solana, D. C. Gulhan, J. G. Milhano, D. Pablos, and K. Rajagopal, J. High Energy Phys. 09 (2015) 175.

[43] J. Casalderrey-Solana, D. C. Gulhan, J. G. Milhano, D. Pablos, and K. Rajagopal, J. High Energy Phys. 03 (2016) 053.

[44] J. Casalderrey-Solana, D. Gulhan, G. Milhano, D. Pablos, and K. Rajagopal, J. High Energy Phys. 03 (2017) 135.

[45] See Supplement Material at http://link.aps.org/supplemental/10.1103/PhysRevLett.128.012301 for a preliminary check on the model dependence of the extraction of χ.

[46] L. Apolinário, N. F. Castro, M. Crispim Romão, J. G. Milhano, R. Pedro, and F. C. R. Peres, arXiv:2106.08869.

[47] A. Białas, M. Bleszyński, and W. Czyż, Nucl. Phys. **B111**, 461 (1976).

[48] M. L. Miller, K. Reygers, S. J. Sanders, and P. Steinberg, Annu. Rev. Nucl. Part. Sci. **57**, 205 (2007).

[49] M. Cacciari, G. P. Salam, and G. Soyez, J. High Energy Phys. 04 (2008) 063.

[50] M. Cacciari, G. P. Salam, and G. Soyez, Eur. Phys. J. C **72**, 1896 (2012).

[51] Additionally, we demand that $p_T > 100$ GeV because this corresponds to the kinematical range where we have trained our neural network. We have also checked that our results do not depend on the precise cut on p_T as long as it is sufficiently below the cut of p_T^{initial}.

[52] U. A. Wiedemann, in *2007 European School of High-Energy Physics* (CERN, Geneva, 2008).

[53] H. Petersen, R. La Placa, and S. A. Bass, J. Phys. G **39**, 055102 (2012).

[54] M. Greif, C. Greiner, B. Schenke, S. Schlichting, and Z. Xu, Phys. Rev. D **96**, 091504(R) (2017).

[55] M. Nie, L. Yi, X. Luo, G. Ma, and J. Jia, Phys. Rev. C **100**, 064905 (2019).

[56] G. Giacalone, B. Schenke, and C. Shen, Phys. Rev. Lett. **125**, 192301 (2020).

[57] M. Gyulassy, I. Vitev, and X.-N. Wang, Phys. Rev. Lett. **86**, 2537 (2001).

[58] X.-N. Wang, Phys. Rev. C **63**, 054902 (2001).

[59] G. Aad, T. Abajyan, B. Abbott, J. Abdallah, S. A. Khalek, R. Aben, B. Abi, M. Abolins, O. AbouZeid, H. Abramowicz *et al.* (ATLAS Collaboration), Phys. Rev. Lett. **111**, 152301 (2013).

[60] T. Lappi, B. Schenke, S. Schlichting, and R. Venugopalan, J. High Energy Phys. 01 (**2016**) 061.

[61] M. Mace, V. V. Skokov, P. Tribedy, and R. Venugopalan, Phys. Rev. Lett. **121**, 052301 (2018).

[62] C. Zhang, C. Marquet, G.-Y. Qin, S.-Y. Wei, and B.-W. Xiao, Phys. Rev. Lett. **122**, 172302 (2019).

[63] J. L. Albacete, H. Petersen, and A. Soto-Ontoso, Phys. Rev. C **95**, 064909 (2017).

[64] F. Gelis, G. Giacalone, P. Guerrero-Rodríguez, C. Marquet, and J.-Y. Ollitrault, arXiv:1907.10948.

[65] B. Blok, C. D. Jäkel, M. Strikman, and U. A. Wiedemann, J. High Energy Phys. 12 (**2017**) 074.

[66] B. Blok and U. A. Wiedemann, Phys. Lett. B **795**, 259 (2019).

[67] In principle, given the absence of energy loss in colorless particles, the value of v_2 for high-p_T photons [68] or Z^0 bosons should also be sensitive to such initial-state induced anisotropy.

[68] A. M. Hamed (STAR Collaboration), Nucl. Phys. **A931**, 706 (2014).

[69] J. G. Milhano and K. C. Zapp, Eur. Phys. J. C **76**, 288 (2016).

[70] A reasonable estimate of the amount of medium induced modification can also be obtained from the ratio between the jet p_T and that of a recoiling colorless trigger boson, although the correlation is not tight even in vacuum due to sizeable out-of-cone radiation [20].

[71] J. Brewer, J. G. Milhano, and J. Thaler, Phys. Rev. Lett. **122**, 222301 (2019).

[72] A. Takacs and K. Tywoniuk, J. High Energy Phys. 10 (2021) 038.

[73] L. Yan, S. Jeon, and C. Gale, Phys. Rev. C **97**, 034914 (2018).

[74] Y. Tachibana, C. Shen, and A. Majumder, arXiv:2001.08321.

[75] J. Casalderrey-Solana, J. G. Milhano, D. Pablos, K. Rajagopal, and X. Yao, J. High Energy Phys. 05 (2021) 230.